



1                   **Warm tropical oceans and ENSO flavours behind the late Holocene change in**  
2                   **hydroclimates in northern South America**

3                   Juan Mauricio Bedoya<sup>1</sup>, Maria I. Velez<sup>2\*</sup>, German Poveda<sup>3</sup>

4                   1.Grupo de Investigación Ingeniería, Facultad de Ciencias Básicas e Ingeniería, Corporación Universitaria Remington, Calle 51 No. 51-27,  
5                   Medellín, Colombia

6                   2.Department of Geology, University of Regina, SK. 3737 Wascana Parkway Regina Sk S4S 0A2

7                   3.Departamento de Geociencias y Medio Ambiente, Universidad Nacional de Colombia, Medellín, Colombia

8                   \* Corresponding author [maria.velez.caicedo@uregina.ca](mailto:maria.velez.caicedo@uregina.ca)

9  
10  
11  
12  
13  
14  
15  
16  
17  
18  
19  
20  
21  
22  
23  
24  
25  
26  
27  
28  
29  
30  
31  
32  
33  
34  
35  
36  
37



38

39      **Abstract**

40    At about 4,000 years ago the earth's global climate underwent significant transformations  
41    resulting from changes in solar insolation. Manifestations of this change are relatively well  
42    known in higher latitudes, however, in the American tropics these are still not fully identified or  
43    understood. Recent paleo-environmental reconstructions based on paleolimnological and  
44    vegetational histories of two Colombian Andean sites suggest that between ~4,150 and 2,500 yr  
45    BP the Eastern Cordillera (EC) witness wetter anomalies, while the Western Cordillera (WC)  
46    suffered from drier anomalies between ~3,700 and 1,750 yr BP. Results from analyses of modern  
47    precipitation series from weather stations close to the study sites indicate that the long-term mean  
48    annual cycle of precipitation in both sites is out-of-phase and that precipitation anomalies on the  
49    western (eastern) site are negatively (positively) correlated with sea surface temperatures in the  
50    tropical Pacific (Tropical Atlantic). Hence that we propose that both oceans warmed up during  
51    the late Holocene, likely from a more active ENSO and ENSO flavours. With the current global  
52    rise in atmospheric temperature and the warming of tropical oceans, this study sheds light on  
53    possible anomalous effects on precipitation over the northern Andes.

54

55

56

57

58

59

60

61

62

63

64

65

66

67

68

69

70

71

72



## 73      **1. Introduction**

74      At around 4,000 years ago, the Earth's global climate experienced a reconfiguration resulting  
75      from changes in insolation and the warming of the Southern Hemisphere (Wanner et al., 2008).  
76      Paleoclimatic reconstructions have provided evidences about some of the consequences of this  
77      change: the cooling of the Atlantic Sea Surface Temperatures (SST) and a shift to the negative  
78      phase in the North Atlantic Oscillation (NAO) and the onset of seasonality in the North  
79      American Prairies (Schwalb et al., 2010), a switch in the forcing of the North American  
80      Monsoon from the Atlantic to the Pacific (Jones et al., 2015), a decrease in intensity of the Indian  
81      Monsoon (Dixit et al., 2014), climate amelioration and diet changes in peoples from the high  
82      Andes Puna (Pintar and Rodriguez, 2022), higher variability in the latitudinal migration of the  
83      Intertropical Convergence Zone (ITCZ) (Sachs et al., 2018) with an overall migration to the  
84      south (Seillès et al., 2016; Ledru et al., 2022), increased precipitation variability in the Caribbean  
85      (Cariaco) (Haug et al., 2001), and a warming of the Tropical Pacific (TP) and the intensification  
86      of the El Niño Southern Oscillation (ENSO) (Toth et al., 2012, Toth and Aronson, 2019; Seillès  
87      et al., 2016; Renseen, 2022), among others. Recent climate models suggest that the location of  
88      seas surface anomalies in the TP, known as ENSO flavours, may have had a great influence over  
89      precipitation anomalies, thus that ENSO flavours may account for conflicting paleoclimatic  
90      reconstructions regarding ENSO during the Holocene (Karamperodou and DiNezio, 2022).

91      In Colombia, late Holocene pollen records have suggested that around 4,000 calibrated years  
92      Before Present (yr BP) climates turned more variable (Marchant et al., 2001) and eventually  
93      became more humid (Marchant and Hooghiemstra, 2004). Recent multiproxy paleolimnological  
94      and paleoclimatic reconstructions from two strategic sites in Colombia have shed new light on  
95      the manifestations of this global event in northern South America. One of the “paleo” records  
96      comes from Santurbán-Berlín, a high-altitude dry paramo in the Eastern Cordillera (EC), and the  
97      other one is from a mid-altitude wetland, Medellincito, in the Western Cordillera (WC), and  
98      close to one of the rainiest places on Earth, the western foothills of the WC (Fig. 1) (Poveda and  
99      Mesa, 2000; Yepes et al., 2019). These reconstructions indicate that Santurbán-Berlín, became  
100      wet between 4,150 and 2,500 yr BP (Patiño et al., 2020) while Medellincito witnessed very dry  
101      conditions between 3,700 and 1,750 yr BP (Jaramillo et al., 2021). This is, eastern Colombia  
102      became wet, while the western part turned dry. This response in hydroclimates to the late



103 Holocene global change warrants some discussion, not only due to its antiphase character but  
104 also because today, average precipitation in Colombia decreases from the west to east (Fig. 1). In  
105 this study, we aim to shed light on the effects and manifestations of the 4 ky BP climate event in  
106 the tropics based on analyses of today's hydroclimates and to contribute to understand the  
107 complex responses of tropical hydroclimates to global phenomena, and thus inform about  
108 possible future climate scenarios resulting from warming oceans based on paleo-climate  
109 inferences.

## 110 **2. Modern hydroclimates of Colombia**

111 Colombia's main sources of atmospheric moisture include the Caribbean Sea, the tropical North  
112 Atlantic and the far eastern Pacific oceans, and also the Amazon region (Arias et al., 2021).  
113 Spatial variability of rainfall (magnitude/phase) is controlled mainly by the presence of the three  
114 branches of the Andes, splitting the country into five distinctive hydroclimatic and ecological  
115 regions, namely: Caribbean, Andean, Pacific, Orinoco and Amazon (Eslava, 1993; Poveda et al.,  
116 2006; Alvarez et al., 2011; Urrea et al., 2019). Diverse mechanisms and processes contribute to  
117 explain the temporal variability of climate and related variables such as rainfall; e.g. the annual  
118 variability is not only controlled by the meridional oscillation of the Intertropical Convergence  
119 Zone (ITCZ), but by its interactions with low-level jets and aerial rivers (Poveda et al., 2006;  
120 2014), while the inter-annual variability is mainly determined by the two phases of El Niño-  
121 Southern Oscillation (ENSO): El Niño (warm phase) and La Niña (cold phase), through ocean-  
122 land-atmosphere interactions and atmospheric teleconnections, regional low-level jets, and land-  
123 surface atmosphere feedbacks and moisture recycling (Bedoya-Soto et al., 2018, 2019, 2019a;  
124 Poveda et al., 2005, 2006, 2020; Cai et al., 2020; Builes-Jaramillo et al., 2018, 2022), discussed  
125 below.

### 126 **2.1 Ocean-atmosphere interactions**

127 Annual precipitation in the Andean region has a bimodal distribution due to the seasonal north-  
128 south migration of the ITCZ (Espinoza et al., 2020; Arias et al., 2021). At decadal, centennial,  
129 and millennial scales, the ITCZ's average latitudinal position, dictated by the location of the  
130 warmer hemisphere, has been the main agent controlling the distribution and intensity of regional  
131 precipitation in northern South America (Haugh et al., 2001; Byrne et al., 2018; Cai et al., 2020).



132 The latitudinal migration of the ITCZ is affected by its interaction with other climatic  
133 phenomena such as the Pacific Decadal Oscillation (PDO), ENSO, and the Atlantic Multidecadal  
134 Oscillation (AMO) (Trenberth and Hurrell 1994; Moy et al., 2002). For instance, in 2010 the  
135 ITCZ was forced to a more northward position due to a warmer than normal Tropical North  
136 Atlantic (TNA) which significantly decreased precipitation in Northeast Brazil, triggering  
137 droughts and affecting moisture storage in the Amazon Basin (Builes et al., 2018; Marengo and  
138 Espinoza, 2016; Cai et al., 2019-2020).

139 ENSO is the most important phenomena inducing climate anomalies at interannual timescales in  
140 northern South America (Poveda et al., 2006; Cai et al., 2020). It also affects the global climate  
141 system in several ways, but mainly through forcing modes in the Atlantic, Indian and Pacific  
142 oceans via atmospheric circulation which in turn trigger different pantropical teleconnections  
143 that finally end up modulating the amplitude, spatial structure, and evolution of warm (El Niño)  
144 and cold (La Niña) phases of ENSO (Poveda et al., 2001, 2006, 2011; Cai et al., 2019, 2020;  
145 Sulca et al., 2018; Espinoza et al., 2020). These changes from event to event known as *ENSO*  
146 *flavours or ENSO diversity* (Tedeschi et al., 2013; Capotondi et al., 2015; Andreoli et al., 2017;  
147 Cai et al., 2020) explain why not all ENSO events and their associated impacts are similar. These  
148 flavours are in turn affected by the interaction between ENSO and other macroclimatic  
149 phenomena such as the PDO, the IPO and the AMO, but also by the location of the main sea  
150 surface temperature (SST) anomalies over the tropical Pacific, so that the response to ENSO in a  
151 given region is different if the core of the anomaly is located in the Eastern Pacific (EP) or in the  
152 Central Pacific (CP). For instance, moisture convergence during La Niña in the Northern Andes  
153 is higher when the SST anomaly occurs in the EP than when it occurs in the CP (Cai et al., 2019,  
154 2020). ENSO and its flavors constitute other important phenomena that affect the climate in  
155 Colombia at interannual scales. Overall, in most of Colombia, El Niño (La Niña) is generally  
156 associated with an increase (decrease) in air temperatures, and with negative (positive) rainfall  
157 anomalies (Poveda et al., 2001).

## 158 **2.2 Ocean-land-atmosphere interactions**

159 Another important source of annual rainfall variability is the interaction between the ITCZ with  
160 atmospheric rivers or diverse low-level jets (LLJs, Fig.1) (Poveda and Mesa, 1999; Poveda et al.,



161 2014; Durán-Quesada et al., 2017; Espinoza et al., 2020; Gimeno et al., 2020). In Colombia these  
162 include the Chocó (over the far eastern Pacific) (Poveda et al., 2000, 2014; Arias et al., 2015;  
163 Hoyos et al., 2018; Bedoya-Soto et al., 2019a; Yepes et al., 2019; Sierra et al., 2021), the  
164 Caribbean (Poveda and Mesa, 1999; Whyte et al., 2008; Muñoz et al., 2008; Cook et al., 2010),  
165 and the Orinoco LLJs (Jimenez-Sánchez et al., 2019; Martinez et al., 2022; Builes et al., 2022),  
166 which is strongly connected with the South American LLJ (Espinoza et al., 2020).

167 Today, the Caribbean and the Chocó LLJs converge into the ITCZ precisely over western  
168 Colombia around 5°N (Poveda and Mesa, 2000), whereas the Orinoco LLJ is blocked and  
169 deviated to the south-east by the EC (Fig. 1). Both the Caribbean and the Chocó LLJs vary  
170 seasonally, and affect the flux of moisture to the foothills of the EC and WC (Poveda et al.,  
171 2014; Hoyos et al., 2018). During the austral summer (DJF), the ITCZ is at its southernmost  
172 position and, consequently, the Orinoco LLJ peaks (maximum winds but minimum rainfall rates)  
173 while the Chocó LLJ is weak. During the boreal summer (JJA), the ITCZ migrates to its  
174 northernmost position, and consequently the Caribbean LLJ peaks while the Orinoco LLJ  
175 weakens (minimum winds but maximum rainfall rates). During this season, and favored by a  
176 strong Caribbean LLJ located north, the Andes are showered by moisture exported from the  
177 Amazon Basin and transported by the inter-cross equatorial flows (Fig. 1) (Salas et al., 2020).  
178 The Chocó LLJ intensifies during the transit of the ITZC from its northern to its southernmost  
179 position during September-October (Poveda et al., 2020).

180 Moreover, local precipitation is affected by the interaction of the aforementioned LLJs, the  
181 tropical easterlies and the complex orography of the Colombian Andes (Trojer, 1959; López and  
182 Howell, 1966; Poveda et al., 2005; Giovannettone and Barros, 2009; Posada-Marín et al., 2018;  
183 Bedoya-Soto et al., 2019a; Espinoza et al., 2020). For instance, the rainiest places in Colombia  
184 such as the foothills of the western slope of the WC and the eastern slopes of the EC and CC are  
185 commonly associated with the blocking of moisture carried by LLJs and synoptic disturbances  
186 with the Andes (Poveda 2000; Poveda et al., 2014; Espinoza et al., 2020). The fate of the  
187 atmospheric moisture transported by the Chocó LLJ is western Colombia including the WC's  
188 foothills, however when it is at its peak, it transports moisture inland crossing the WC (Poveda  
189 et al., 2014; Gimeno et al., 2020). Conversely, the fate of the atmospheric moisture carried by the

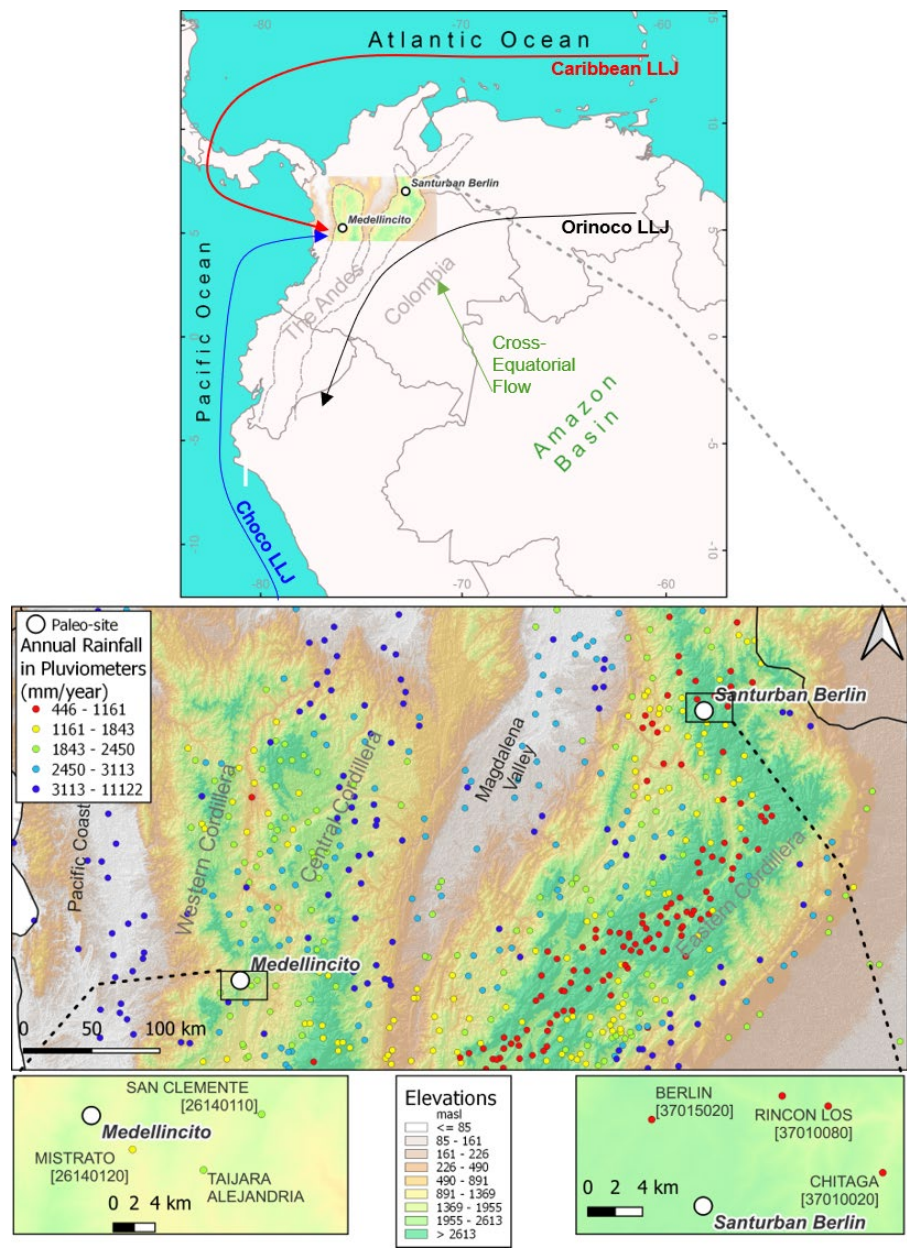


190 Orinoco LLJs and the Easterlies is the eastern flank of the EC. All this implies that seasonal  
191 precipitation on EC and WC is affected in multiple ways.

### 192 **2.3 Land-atmosphere**

193 Moisture generated over land is recycled vertically through evapotranspiration-precipitation  
194 fluxes and horizontally through advected cascades that connect with the vertical ones (Zemp et  
195 al., 2014, 2017). For instance, the Magdalena River valley that divides the EC and CC (Fig. 1), is  
196 an important source of moisture from evaporation to higher sites on these cordilleras (Hoyos et  
197 al., 2018; Bedoya-Soto et al., 2019a; Escobar et al., 2022).





198  
199  
200 Figure 1. Colombia’s main sources of moisture and trajectory of main LLJs. Paleo-study sites in  
201 the highlighted square (top). Detail of the shaded area showing mean annual rainfall distribution  
202 (mm/year in coloured dots) over the Andes (for the period 1976-2015) and location of the closest  
203 weather stations to the “paleo” sites (bottom).





### 205 3.Methods

206 The two “paleo” environmental reconstructions are based on the record from Santurbán-Berlín  
 207 (7° 6.6’N, 72° 49’W at 3,800 m asl) that covers the last 27,000 yr BP, and studied using diatoms,  
 208 litho-stratigraphy and element concentrations (Patiño et al., 2020), and the record from  
 209 Medellín (5° 19’N, 75° 54’W at 2000 m asl) almost 7,000 years old interrupted by one hiatus  
 210 from 3,710 to 1,560 yr BP, and analyzed using diatoms, isotope geochemistry, litho-stratigraphy  
 211 and pollen (Jaramillo et al., 2021). The age models presented here are taken from the original  
 212 articles (where they are discussed at length), based on Bayesian statistics of fifteen and eight <sup>14</sup>C  
 213 dates for Santurbán-Berlín and Medellín, respectively, processed through Bacon software  
 214 (Blaauw and Christen, 2011). Here we present all ages as calibrated ages.

215 Modern hydroclimate information for the two “paleo” sites was obtained from the national rain  
 216 gauge network operated by IDEAM, the Colombian Hydrological and Meteorological Institute  
 217 (<http://dhime.ideam.gov.co>) for Mistrató and Berlín, the nearest meteorological stations to  
 218 Medellín and Santurbán-Berlín respectively (Fig. 1, Table 1). We used monthly rainfall  
 219 series ranging from 1976 to 2015 and decomposed them using a Seasonal Decomposition of  
 220 Time Series by Loess (STL) (Cleveland et al., 1990). The STL is based on eigenvalue and  
 221 frequency response analysis. The seasonal component is the annual cycle, the trend component  
 222 represents the low-frequency variability including non-stationarities, and the remainder  
 223 component is the difference between seasonal and trend components (stochastic). All was  
 224 computed using “R” (R Core Team, 2021).

225 Table 1. Information of the meteorological stations used in this study

Pluviometer Name (ID Code)	Distance to “paleo” site	Vegetation	Lat (°N)	Lon (°W)	Elev (m)	Source
Mistrató (26140120)	10 km Medellincito	Andean Forest	5.29425	75.872	1483	IDEAM
Berlín (37015020)	4 km, Sant.-Berlín	Paramo	7.18694	72.8686	3214	IDEAM



227 The trend component associated to the interannual variability for the two stations was correlated  
 228 with: (i) global SST (HADISST; <https://www.metoffice.gov.uk/hadobs/hadisst/>) and (ii) the Total  
 229 Column of Water (TCW; extracted from the ERA5 reanalysis  
 230 (<https://www.ecmwf.int/en/forecasts/datasets/reanalysis-datasets/era5>) to elucidate the possible  
 231 effects of both the Pacific and tropical North Atlantic SSTs variability on interannual and  
 232 interdecadal precipitation over the two study sites, and to identify other possible agents of rainfall  
 233 and moisture variability at global, regional, and local scales (Table 2). These correlations were  
 234 estimated using KNMI Climate Explorer (<https://climexp.knmi.nl/>).

235 The parcel trajectory online software *traj3d* (based on the NCAR/NCEP Reanalysis I) was used  
 236 for the backward tracking of the sources of air moist parcels arriving to the study sites, in a  
 237 Lagrangian model. This model was obtained from the University of Melbourne Parcel Trajectory  
 238 Software (<http://www.cycstats.org/trajectories/trajhome.htm>) and run at 700 mb for October 2010,  
 239 an anomalously wet month enhanced by La Niña. A discussion of the algorithm is given by Noone  
 240 and Simmonds (1999) and Barras and Simmonds (2009).

241 Table 2. Sources for the global climate data used

242

Climate Data	Period	Data Source	Reference	Source
Sea Surface Temperature (SST)	1871-2022	HADISST	MetOffice	KNMI Climate Explorer
Total Column of Water (TCW)	1950-2022	ERA5	Hersbach et al., 2020	

243

244 The wavelet transform was used to quantify the temporal variability of spectral properties of  
 245 monthly rainfall time series and the temporal cross-coherence between their phases (Daubechies,  
 246 1990; Torrence and Compo, 1998). We estimate the wavelet transforms, as well as the wavelet  
 247 coherence between the monthly series of rainfall at both study sites, to identify the epochs and  
 248 frequencies that explain the highest portion of the variance between both series, and also their  
 249 coherence, in order to identify when they were in and out of phase. For practical purposes we  
 250 employed the continuous wavelet transform (CWT) (Torrence and Compo, 1998) and the cross-



251 wavelet analysis (CWA) (Maraun and Kurths, 2004) that involves the wavelet cross-spectrum  
252 (WCS), which is defined as the expected value of the product of the single wavelet power spectra  
253 of both time series at a certain time, on a scale  $s$ . We used the Morlet complex wavelet, consisting  
254 of a plane wave modulated by a Gaussian, which provides diverse advantages with respect to other  
255 wavelets (Yi and Shu, 2012). It was implemented using *waipy*, a python package developed by  
256 Mabel C. Costa, available at <https://github.com/mabelcalim/waipy>, accessed on October 2, 2022.  
257

## 258 **4. Results**

### 259 **4.1. Study sites' modern hydroclimates controls**

260 Today, annual rainfall in the Colombian Andes decreases from west to east, and upslope, so that  
261 mid altitude sites on the WC such as Medellincito (2,000 masl) are generally humid, while high  
262 elevation sites on the EC such as Santurbán-Berlín (3,800 m asl) are drier (Fig. 1).

#### 263 **4.1.1 Annual scale of hydroclimate variability**

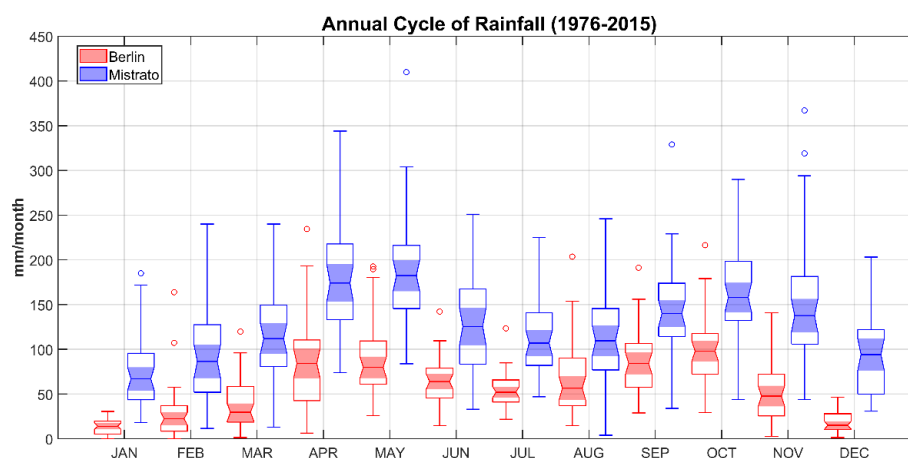
264 Medellincito (Mistrató station), lies under the moisturizing-air flow of the Chocó LLJ, the  
265 recycling of moisture from the Chocó rainforest, and the interaction between the Chocó LLJ and  
266 the WC (Figs. 1,2) (Jaramillo et al., 2021). The annual cycle of rainfall is bimodal with two  
267 humid (Apr-May and Oct-Nov) and two drier periods (Jun-Jul-Aug and Dec-Jan-Feb) following  
268 the seasonal trajectory of the ITCZ (Poveda et al., 2014). This annual cycle ranges between 75  
269 and 180 mm/month with an annual mean rainfall of 1564 mm (Fig. 2).

270 In the area of Santurbán-Berlín, the annual cycle of rainfall varies from unimodal, mainly in the  
271 eastern slope, to bimodal in the western slope. In Berlín station, close to the watershed divide,  
272 the annual cycle is specifically bimodal with 696 mm of mean annual rainfall, with maxima  
273 during October (150 mm/month) and April (175 mm/month), and minima during January (60  
274 mm/month) and July (100 mm/month) (Fig. 2).

275 Results of the wavelet spectrum of monthly rainfall series at Mistrató and Berlín (Fig. 3 a-b)  
276 indicate a much sharper and more predominant semi-annual cycle at Mistrató (WC) and a much  
277 weaker signal at the annual timescale, while in Berlín (EC), the annual cycle exhibits a stronger  
278 and broader signal than the semi-annual. The cross-power spectra among both time series (Fig. 3c)



279 shows an almost non-existent coherence among both rain gauges at semi-annual and annual  
280 timescales through the study period. These results indicate that, in spite of the bimodal character  
281 of the annual cycle of precipitation at both sites they respond to different processes and  
282 mechanisms, beyond the meridional oscillation of the ITCZ over northern South America at annual  
283 and semi-annual timescales.



284

285 Figure 2. Long-term mean annual cycle of rainfall at Mistrató on the western Andes (blue) and  
286 Berlin on the eastern Andes (red).

287

288

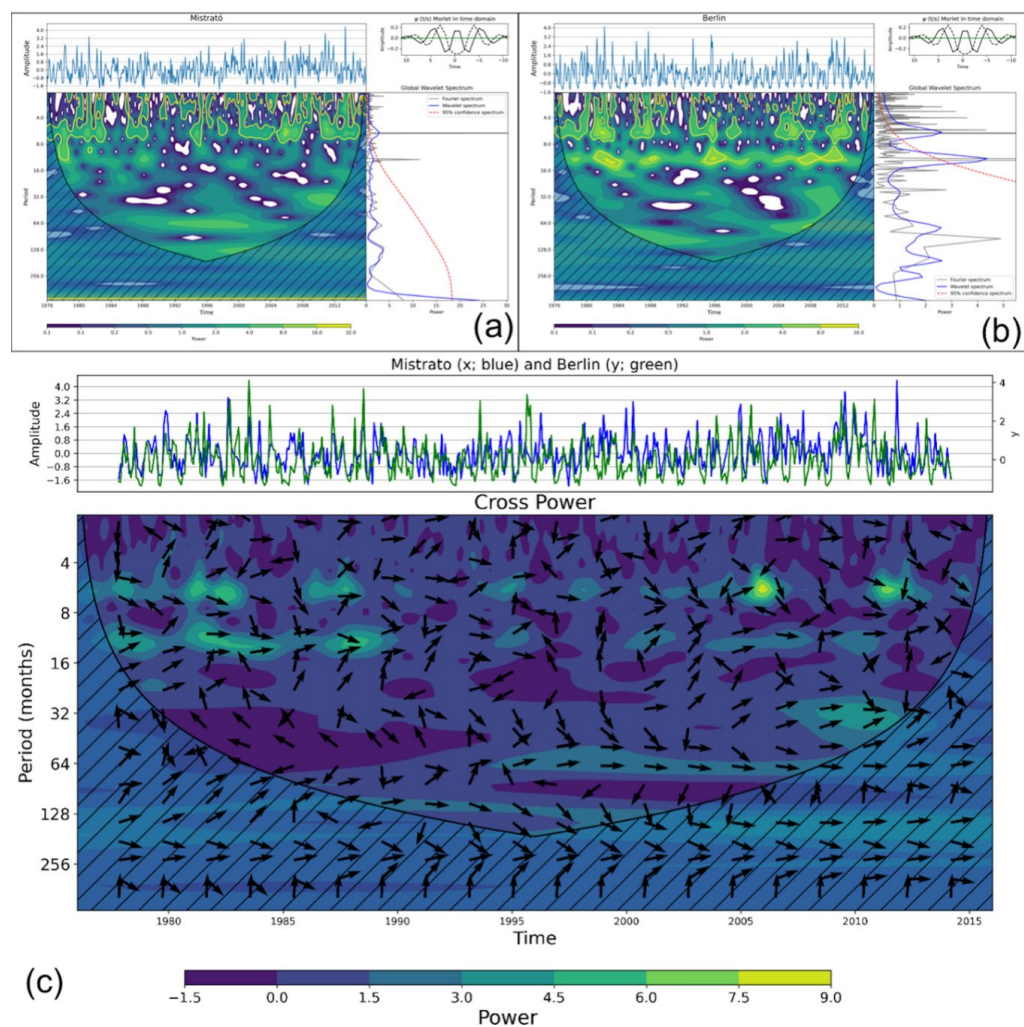


Figure 3. Wavelet spectrum of the monthly rainfall series at Mistrató on the WC (a) and Berlin over the EC (b), along with the cross-power spectra among both series (c).

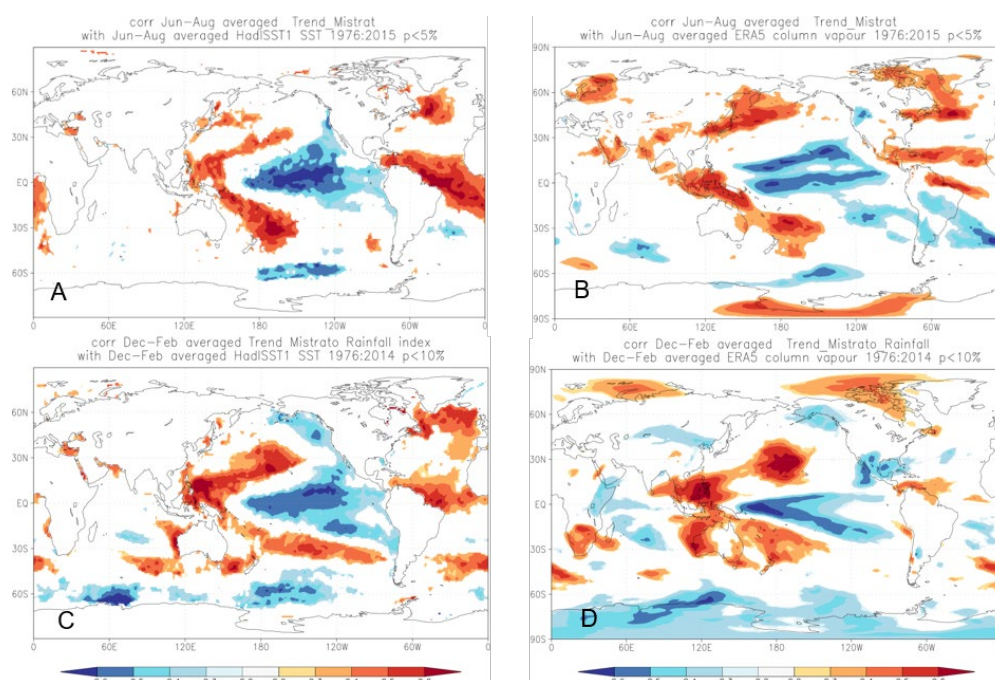
#### 4.1.2 Interannual scale of hydroclimate variability

Monthly time series were decomposed using the STL into the seasonal component, which reflects the annual cycle, the trend component, which reflects variability in precipitation at



297 interannual scales, and the remainder component which is the residual after extracting the  
298 seasonal and trend components from each monthly series.

299 Decomposition results of precipitation series at Mistrató located on the western Andes are  
300 presented in Fig S1 (Supplementary Information). Correlations between the trend component with  
301 global SSTs (Fig. 4 A, C) and TCW (Fig. 4 B, D) show that during June-July-August, the trend  
302 component is negatively correlated with SSTs over the Central TP ( $r < -0.6$ ,  $p > 0.05$ ) and  
303 positively correlated with SSTs over the TNA ( $r > 0.6$ ,  $p > 0.05$ , Fig 4A). This means that El Niño-  
304 like warm waters in the TP (TNA) are associated with a decrease (increase) in precipitation at  
305 Mistrató (Berlín). Correlations with the TCW depict zonal and meridional moisture flows coming  
306 from the TP, TNA, and a cross-equatorial moisture flow coming from the Amazon-Andes (Fig. 4  
307 B, D). The latter acts via the latitudinal migrations of the South Atlantic Convergence Zone (Hu  
308 and Fedorov, 2018) (Fig. 4B).



309

310





Figure 4. Global seasonal correlation maps for Mistrató using the trend component for SSTs (HADISST) and TCW (ERA-5) during the boreal summer, June-August (A-B) and during the austral summer December-February (C-D)

Decomposition results of precipitation series in Berlín located over the eastern Andes are presented in Fig. S2 (Supplementary Information). Correlation analyses of the trend component with global SSTs (Fig. 5 A,C) and TCW (Fig. 5 B,D) indicate that precipitation is positively correlated with SST in the TNA, particularly during the boreal summer when the ITZC is at its the northernmost position (Fig. 5 A,B) ( $r = 0.6, p > 0.05$ ). This means that when the TNA warms up interannually, precipitation in Santurbán-Berlín increases, owing to the zonal effect of available TCW which is constrained to the zonal wind flow including direct connections with the TNA region (Fig. 5B).

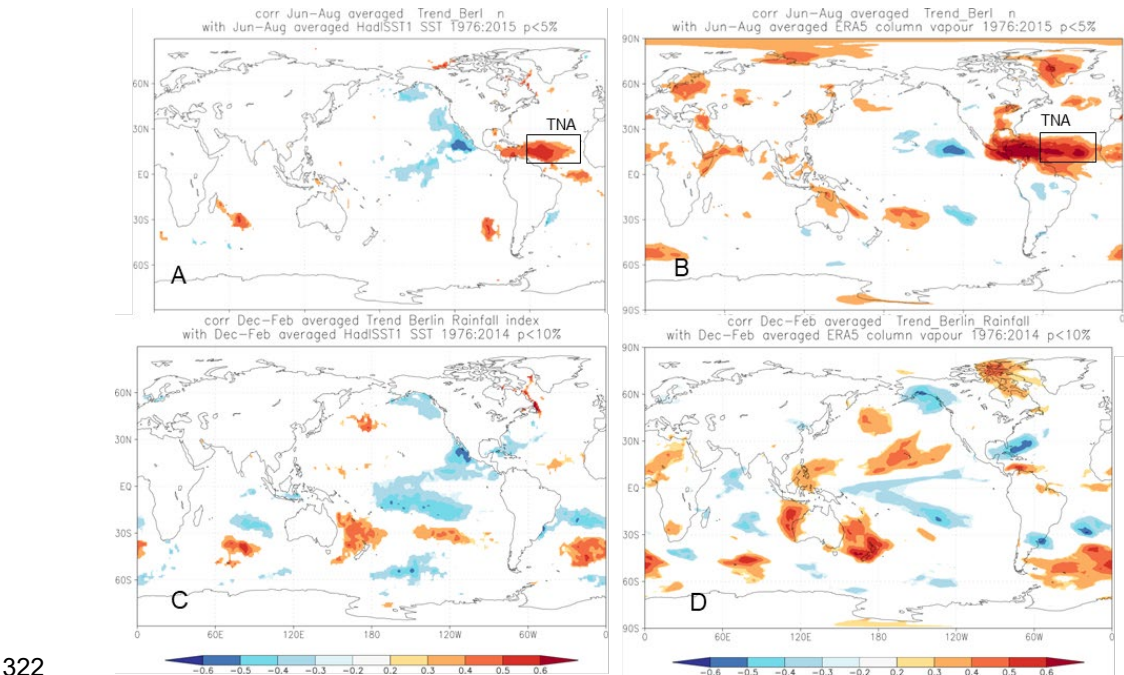


Figure 5. Seasonal correlation maps in Berlín station using the trend component for global SSTs (HADISST) and TCW (ERA-5) during the boreal summer, June-August (A-B) and during the austral summer, December-February (C-D)





Results of the backward-Lagrangian tracking analysis of air parcels at 700 mb for the study sites during a humid period of the annual cycle enhanced by La Niña (October 2010) are presented in Fig. 6. Parcels ending in Berlín originated in the TNA region, traveled predominantly east-west crossing the northernmost part of continental South America before entering Colombia through the north east (Fig. 6A). Air parcels ending in Mistrató, originated in southeastern Pacific and travelled from south to north and east to west just before entering Colombia through the west (Fig. 6B). In spite that both sites are closely located and interconnected by the influence of the three ranges of the Andes, the origin of humid parcels and the physical mechanisms governing rainfall at both sites differ at seasonal and interannual timescales.

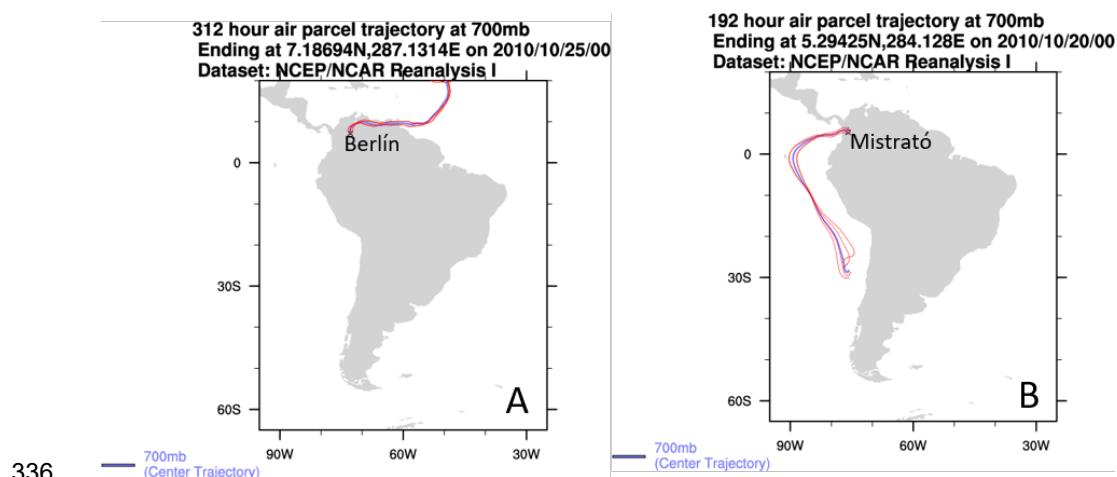
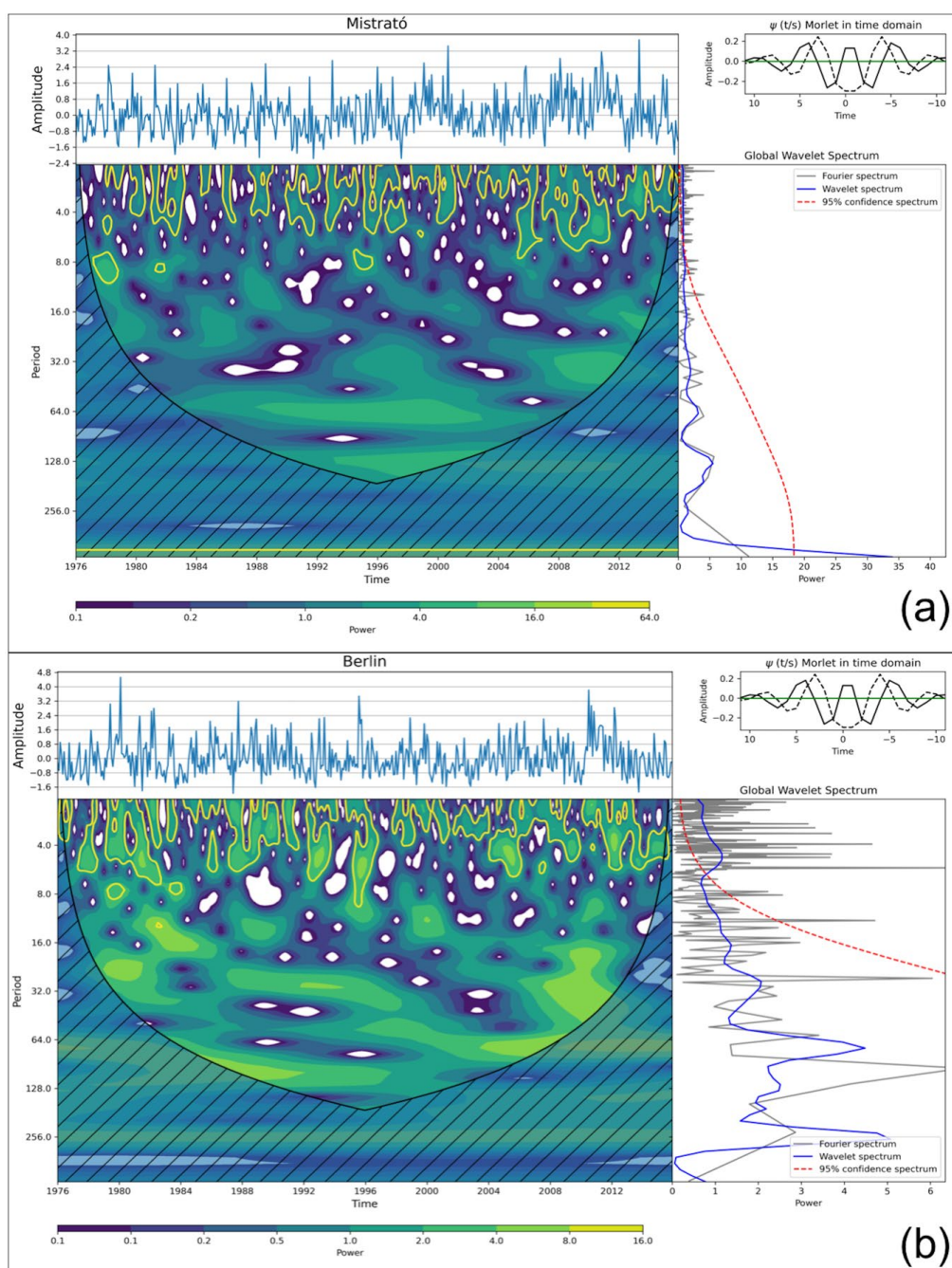


Figure 6. Backward Lagrangian air parcel-tracking during La Niña of October 2010 (an anomalous wet year), showing the different moisture sources at Berlín and Mistrató (6A and 6B, respectively). Image provided by the NOAA Physical Sciences Laboratory, Boulder Colorado from their web site at <https://psl.noaa.gov/>

Results of the wavelet analyses at interannual timescales are shown in Figure 7, using the standardized time series at both study sites. As expected, the wavelet spectra at both sites (Figs. 7a and 7b) no longer exhibit significant, strong and well-defined peaks at semi-annual and annual timescales, but a broader signal at interannual timescales, being weaker (stronger) at Mistrató

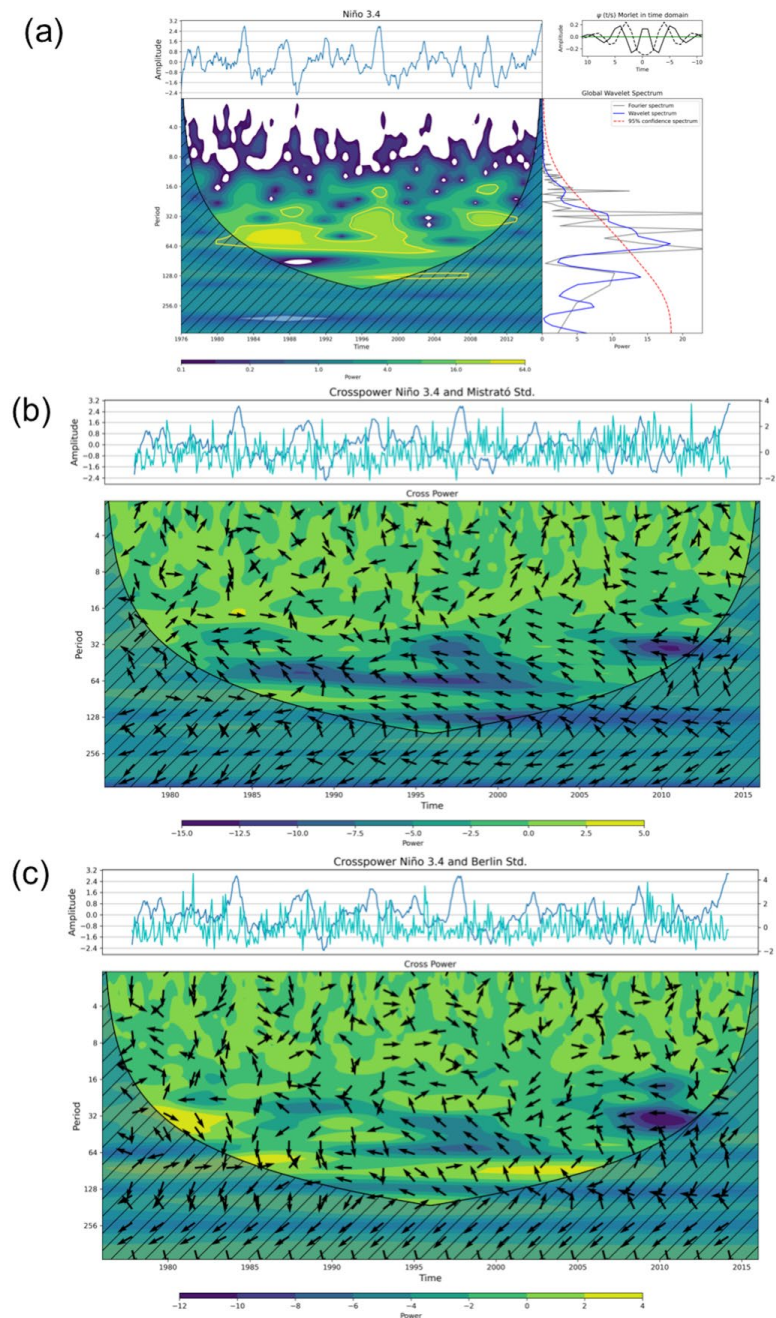


(Berlín). The cross-power spectrum (not shown) among the standardized rainfall series at both rain gauges shows a rather weak coherence at interannual timescales (~64 months), but localized in time from 1998 onwards. Given that ENSO is the most important mechanism driving the hydroclimatology of these two Colombian regions, it is relevant to quantify the wavelet power spectrum of the Niño 3.4 index (Fig. 8a), one of the main indices of ENSO, and its cross-power spectra with the standardized rainfall series at Mistrató and Berlín (Figs. 8 b,c). As expected, the wavelet spectrum of the Niño 3.4 monthly series exhibits a broad-band global wavelet spectrum with a stronger signal between 28-64 months, and some other decadal timescales (~128 months). Interestingly, the global wavelet spectrum shows a sharp decrease between 64 and 168 months. The cross-spectra between El Niño 3.4 index monthly series and the standardized precipitation series at Mistrató shows an out-of-phase behavior at 32 months (1995-2015), at 64 months (1985-2005), and longer timescales during the whole study period, albeit most outside the significative cone of influence, which implies that an increase in SSTs in the Central Pacific is associated with negative rainfall anomalies at Mistrató at interannual timescales. On the other hand, the cross-spectra between El Niño 3.4 index and the monthly standardized rainfall series at Berlín (Fig. 8c) shows a coherent in-phase behavior, in particular in the frequency band spanning from 64 to 90 years, which confirms that positive interannual SST anomalies in the Central Pacific (El Niño) is associated with positive rainfall anomalies at Berlin. Similar analyses between the monthly series of the TNA and the monthly standardized rainfall series at both study sites indicate that the TNA exhibits a strong multidecadal signal around 90-100 years (Fig. 9a), and an almost constant out-of-phase association with monthly standardized rainfall at Mistrató (Fig. 9b), mainly from interannual to interdecadal (30-90 years) timescales, which also confirms that positive anomalies in the TNA index are associated with negative rainfall anomalies at Mistrató at interdecadal timescales. On the other hand, the cross-spectra between the TNA and standardized rainfall at Berlin (Fig. 9c) exhibit a coherent in-phase association, mainly at 64-yr and longer timescales, which also confirms that positive anomalies in the TNA are associated with positive anomalies at Berlín at interdecadal timescales.



374

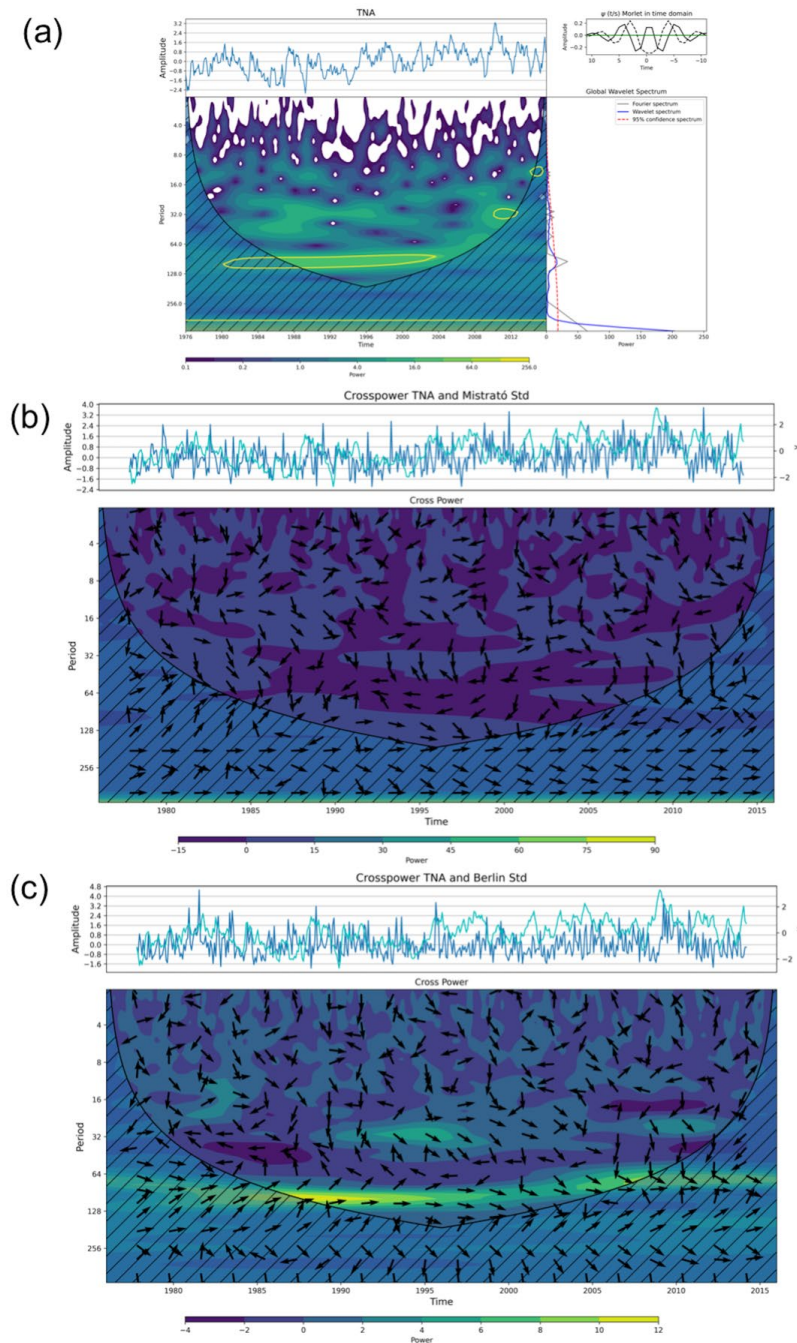
375 Figure 7. Wavelet spectrum of the standardized monthly rainfall series at Mistrató on the WC (a),  
376 and Berlín on the EC (b).



377

378 Figure 8. Wavelet spectrum of the monthly series of the Niño 3.4 index (a). Cross power spectra  
379 between the monthly series of the Niño 3.4 index and the monthly standardized rainfall series at  
380 Mistrató and Berlín, respectively (b and c).





381  
382

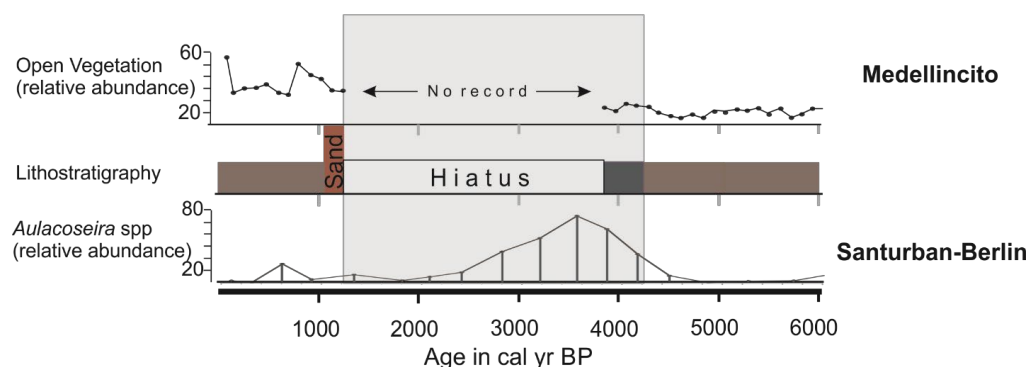
383 Figure 9. (a) Wavelet spectrum of the monthly series of the TNA index (a), Cross power spectra  
384 between the monthly series of the TNA index and the monthly standardized rainfall series at  
385 Mistrató and Berlín, respectively (b and c).



386

## 387 4.2 Paleo-climate archives

388 In Santurbán-Berlín a decrease in detrital input, an increase in lake water levels and or an extension  
389 of the wetland and an increase in runoff, interpreted as an increase in precipitation and wetland  
390 productivity (Patiño et al., 2020) is dated between ~4,150 and lasted ~2,800 yr BP. This change  
391 was inferred from a sharp change in core lithology from pale silt to organic mud, a peak in  
392 *Aulacoseira* spp, a planktonic diatom previously absent from the record, and an increase in Ti:Ca  
393 (Patiño et al., 2020; Fig. 10). In Medellincito-Mistrató, a change to dry conditions was inferred  
394 from a hiatus, an increase in sand content, open vegetation, aerophil diatoms and an excursion in  
395 nitrogen and carbon isotopes (Fig. 10) between ~3700 and 1270 yr. BP (Jaramillo et al., 2021).  
396 The absence of pollen indicative of anthropogenic activity in both records indicates that these  
397 changes are non-anthropogenic and that both sites were affected by natural agents e.g. climate  
398 variability. The climate configuration of Colombia during the late Holocene, wet in the high  
399 elevations of the EC and dry in the WC, are opposite to conditions reigning today (Fig 1).



400

401

402 Figure 10. Records from the “paleo” sites. From bottom to top: relative proportion of planktonic  
403 diatom *Aulacoseira* spp in the record interpreted as increase in precipitation in Santurbán-Berlín.  
404 Lithostratigraphy, hiatus and relative proportion of open vegetation indicating a dry period in  
405 Medellincito-Mistrató. Shaded areas indicate the period of climate change recorded at the two  
406 sites.

407



## 408      **5. Discussion**

409      Results from our analyses indicate that the SSTs and TWC in the TNA and TP have significant  
410      effects on today's precipitation in our study sites (Figs. 4 and 5). In Mistrató, decreases (increases)  
411      in precipitation are correlated with warm waters in the TP (TNA), whereas when the TNA warms  
412      up precipitation increases in Santurbán-Berlín. Our results also confirm that monthly precipitation  
413      at both sites are out of phase, and that the main sources of moisture are the TNA for Santurbán-  
414      Berlín and the tropical Pacific for Medellín-Mistrató. Based on this, we propose that the late  
415      Holocene change in Colombia was caused by the increase in SST in the TNA and TP.

416      The out-of-phase character of the late Holocene climate change in both study sites is confirmed by  
417      other climate inferences. For instance, the Central Cordillera which is affected by moisture coming  
418      from the Chocó LLJ, turned dry between ca. 5,900 and 3,200 yr BP (Berrio et al., 2002), and the  
419      eastern savannas and lake La Cocha, a high-altitude lake on the southern part of EC, became more  
420      humid after about 4,000 cal yr BP (Gonzalez-Carranza et al., 2012; Hooghiemstra and Flantua,  
421      2019). Other paleoclimatic records and climate models have also suggested that TP SSTs warmed  
422      up in the late Holocene (Seillès et al., 2016), and that ENSO events became more frequent and  
423      intensified until about 1800-1200 cal yr BP (Moy et al., 2001; Donders et al., 2008). An increase  
424      in ENSO frequency would explain the late Holocene change to dry conditions in Medellín, but  
425      wouldn't necessarily explain the shift to wetter conditions over the eastern regions of Colombia,  
426      confirming that in addition to the TP becoming warmer, the tropical Atlantic also warmed up, as  
427      suggested by the analysis in this study. The warming of the two tropical oceans during the late  
428      Holocene is explained by ENSO flavors or the pantropical interconnections that occur during some  
429      ENSO events suggesting that in addition to ENSO intensifying, it also became more diverse. This  
430      finding is in agreement with recent climate modelling suggesting that during the late Holocene  
431      event frequency increased in the Eastern Pacific and decrease in the Central Pacific and Coastal  
432      (ENSO flavours) as a result of orbital forcing (Karamperidou and DiNezio, 2022). Today's ENSO  
433      teleconnected regions located either outside or in the tropics started to be more variable at around  
434      5,000 (4,000 cal yr BP), including continental South America (Donders et al., 2008). The increase  
435      in ENSO's frequency and amplitude in the late Holocene is attributed to changes in Northern  
436      Hemisphere's insulation and subsequent changes in the Pacific trade winds (Moy et al., 2008) and  
437      also from extra heating of the Indo Pacific Warm Pool (Donders et al., 2008) that triggered





cyclicality. Generally speaking, ENSO frequency increased after 5,000 yr BP, reached a peak in variability between ca. 3,000 and 1,800 yr BP (1,200 according to Donders et al., 2008) declining afterwards (Moy et al., 2001; Toth et al., 2012, 2019). The change in our records to modern like conditions after 1250 in the WC converges with this pattern (the record from the EC after 2,500 cal yr BP is of very low resolution to be able to record this change).

It has been proposed that during the late Holocene the ITCZ migrated south and maintained a more southern position (Haug et al., 2001; Seillès et al., 2016; Ledru et al., 2022). Our results confirm this as this ITCZ southern shift would have weakened or shifted south the Chocó LLJ reducing moisture in the WC (Mistrató), at the same time that it would have allowed the easterlies to enter the EC (Berlín), increasing precipitation.

In summary, modern analyses of today's precipitation series indicate that precipitation in the study sites is out-of-phase, that the sources of moisture for Berlín (Santurbán-Berlín) and Mistrató (Medellincito) originate in the TNA and the Pacific, respectively, and that interannual variability of the global sources of moisture generated in the TP and TNA modulate the amount of moisture feeding the ITCZ and thus precipitation over the Andes, that with their complex orography, end up altering further local precipitation. Hence that besides the fact that the two "paleo" sites are less than 400 km apart, and that the ITCZ governs precipitation in both sites, there are other factors that induce complexity to the system and end up altering precipitation. TNA and TP have a significant effect on today's precipitation in our study sites (Figs. 4-9).

## Conclusions

Out-of-phase precipitation anomalies in the western and eastern cordilleras of the Colombian Andes during the late Holocene, can be explained by the warming of the Tropical Pacific and Tropical North Atlantic likely from an increase in ENSO and ENSO flavours events.

Given that current global warming is affecting the SST of the tropical oceans and consequently the temperature gradient between the NH and SH, there likely be consequences on the average position of the ITCZ, and precipitation distribution in the Colombian Andes, the most densely populated region of Colombia that depend on the water resources maintained by the current precipitation regimes.



466 **Author contribution**

467 MIV and JMB designed the investigation. MIV supported the “paleo” component of this  
468 research. JMB and GP provided modern hydroclimate analyses. All authors contributed to the  
469 analyses and discussion of results and to the writing of the manuscript.

470 **Competing interests**

471 We declare no competing interests.

472 **References**

- 473  
474 Andreoli, R. V., de Oliveira, S. S., Kayano, M. T., Viegas, J., de Souza, R. A. F., & Candido, L.  
475 A.: The influence of different El Niño types on the South American rainfall, *Int J Climatol* 37,  
476 1374-1390, <http://dx.doi.org/10.1002/joc.4783>, 2017.  
477  
478 Arias, P. A., Martínez, J. A., & Vieira, S. C.: Moisture sources to the 2010–2012 anomalous wet  
479 season in northern South America, *Clim Dynam*, 45, 2861-2884,  
480 <http://dx.doi.org/10.1007/s00382-015-2511-7>, 2015.  
  
481 Arias, P. A., Garreaud, R., Poveda, G., Espinoza, J. C., Molina-Carpio, J., Masiokas, M., Viale,  
482 M., Scaff, L., & van Oevelen, P. J.: Hydroclimate of the Andes part II: hydroclimate variability  
483 and sub-continental patterns, *Front Earth Sci*, 8, 505467.  
484 <http://dx.doi.org/10.3389/feart.2020.505467>, 2021.  
  
485 Barras, V., and Simmonds, I.: Observation and modeling of stable water isotopes as diagnostics  
486 of rainfall dynamics over southeastern Australia, *J Geophys Res* 114, D23308,  
487 <http://dx.doi.org/10.1029/2009JD012132>, 2009.  
488  
489 Bedoya-Soto, J. M., Poveda, G., & Sauchyn, D.: New insights on land surface-atmosphere  
490 feedbacks over tropical South America at interannual timescales, *Water*, 10, 1095-,  
491 <http://dx.doi.org/10.3390/w10081095>, 2018.  
492  
493 Bedoya-Soto, J. M., Poveda, G., Trenberth, K. E., & Vélez-Upegui, J. J.: Interannual  
494 hydroclimatic variability and the 2009–2011 extreme ENSO phases in Colombia: from Andean  
495 glaciers to Caribbean lowlands, *Theor Appl Climatol*, 135, 1531-1544,  
496 <http://dx.doi.org/10.1007/s00704-018-2452-2>, 2019.  
497



- 498 Bedoya-Soto, J. M., Aristizábal, E., Carmona, A. M., & Poveda, G.: Seasonal Shift of the  
499 Diurnal Cycle of Rainfall Over Medellín's Valley, Central Andes of Colombia (1998–2005),  
500 Front Earth Sci 7, 92-, <http://dx.doi.org/10.3389/feart.2019.00092>, 2019a.  
501
- 502 Blaauw, M. and Christen, J.A.: Flexible paleoclimate age-depth models using an autoregressive  
503 gamma process, Bayesian Anal, 6 457–474, <http://dx.doi.org/10.1214/11-BA618>, 2011.  
504
- 505 Byrne, M. P., Pendergrass, A. G., Rapp, A. D., & Wodzicki, K. R.: Response of the intertropical  
506 convergence zone to climate change: Location, width, and strength, Current climate change  
507 reports, 4, 355–370, <http://dx.doi.org/10.1007/s40641-018-0110-5>, 2018.  
508
- 509 Builes-Jaramillo, A., Ramos, A. M., & Poveda, G.: Atmosphere-land bridge between the Pacific  
510 and tropical North Atlantic SST's through the Amazon River basin during the 2005 and 2010  
511 droughts. Chaos: An Interdisciplinary Journal of Nonlinear Science, 28, 085705,  
512 <http://dx.doi.org/10.1063/1.5020502>, 2018.  
513
- 514 Builes-Jaramillo, A., Yepes, J., & Salas, H. D.: The Orinoco Low-Level Jet and its association  
515 with the hydroclimatology of northern South America, Journal of Hydrometeorology, 23, 209–  
516 223, <http://dx.doi.org/10.1175/JHM-D-21-0073.1>, 2022.  
517
- 518 Cai, W., Wu, L., Lengaigne, M., Li, T., McGregor, S., Kug, J. S., ... & Chang, P.: Pantropical  
519 climate interactions, Science, 363,6430, <http://dx.doi.org/10.1126/science.aav4236>, 2019.  
520
- 521 Cai, W., McPhaden, M. J., Grimm, A. M., Rodrigues, R. R., Taschetto, A. S., Garreaud, R. D. &  
522 Vera, C.: Climate impacts of the El Niño–southern oscillation on South America, Nature  
523 Reviews Earth & Environment, 1, 215–231, <http://dx.doi.org/10.1038/s43017-020-0040-3>, 2020.  
524
- 525 Capotondi, A., Wittenberg, A. T., Newman, M., Di Lorenzo, E., Yu, J. Y., Braconnot, P., ... &  
526 Yeh, S. W.: Understanding ENSO diversity, B Am Meteorol Soc, 96, 921–938,  
527 <http://dx.doi.org/10.1175/BAMS-D-13-00117.1>, 2015.  
528
- 529 Cleveland, R. B., Cleveland W. S., McRae J.E., and Terpenning I. STL: A Seasonal-Trend  
530 Decomposition Procedure Based on Loess. J Off Stat, 6, 3–73. 1990  
531
- 532 Córdoba-Machado, S., Palomino-Lemus, R., Gámiz-Fortis, S. R., Castro-Díez, Y., & Esteban-  
533 Parra, M. J.: Influence of tropical Pacific SST on seasonal precipitation in Colombia: prediction  
534 using El Niño and El Niño Modoki. Clim Dynam, 44, 1293–1310,  
535 <http://dx.doi.org/10.1007/s00382-014-2232-3>, 2015.  
536



- 537 Córdoba-Machado, S., Palomino-Lemus, R., Gamiz-Fortis, S. R., Castro-Díez, Y., & Esteban-  
538 Parra, M. J. Assessing the impact of El Niño Modoki on seasonal precipitation in Colombia,  
539 Global Planet Change, 124, 41-61, <http://dx.doi.org/10.1016/j.gloplacha.2014.11.003>, 2015.  
540
- 541 Cook, K. H., & Vizy, E. K.: Hydrodynamics of the Caribbean low-level jet and its relationship to  
542 precipitation, J Climate, 23, 1477-1494, <http://dx.doi.org/10.1175/2009JCLI3210.1>, 2010.  
543
- 544 Daubechies, I.: The wavelet transform time-frequency localization and signal analysis, IEEE  
545 Trans. Inform. Theory, 36, 961–1004, <http://dx.doi.org/10.1109/18.57199>, 1990.  
546
- 547 Dixit, Y., Hodell, D., and Petrie, C.: Abrupt weakening of the summer monsoon in northwest  
548 India ~4100 yr ago, Geology, 42, 339–342, <http://dx.doi.org/10.1130/G35236.1>, 2014.  
549
- 550 Durán-Quesada, A. M., Gimeno, L., & Amador, J.: Role of moisture transport for Central  
551 American precipitation, Earth Sys Dynam, 8, 147-161, [http://dx.doi.org/10.5194/esd-8-147-](http://dx.doi.org/10.5194/esd-8-147-2017)  
552 [2017](http://dx.doi.org/10.5194/esd-8-147-2017), 2017  
553
- 554 Enfield, D.B., Mestas, A.M., Mayer, D.A. and Cid-Serrano, L.: How ubiquitous is the dipole  
555 relationship in tropical Atlantic sea surface temperatures?, JGR-O, 104, 7841-7848,  
556 <http://dx.doi.org/10.1029/1998JC900109>, 1999.  
557
- 558 Eslava, J.: Climatología y diversidad climática de Colombia. Rev. Acad. Colomb. Cien., 18, 507-  
559 538, 1993  
560
- 561 Espinoza, J. C., Garreaud, R., Poveda, G., Arias, P. A., Molina-Carpio, J., Masiokas, M., Viale,  
562 M., & Scaff, L.: Hydroclimate of the Andes Part I: main climatic features, Front Earth Sci, 8, 64-  
563 , <http://dx.doi.org/10.3389/feart.2020.00064>, 2020.  
564
- 565 Escobar, M., Hoyos, I., Nieto, R., & Villegas, J. C.: The importance of continental evaporation  
566 for precipitation in Colombia: A baseline combining observations from stable isotopes and  
567 modelling moisture trajectories, Hydrol Process, 36, 14595, <http://dx.doi.org/10.1002/hyp.14595>,  
568 2022.  
569
- 570 Giovannettone, J. P., and Barros, A. P.: Probing regional orographic controls of precipitation and  
571 cloudiness in the central Andes using satellite data. J Hydrometeorol, 10, 167-182,  
572 <http://dx.doi.org/10.1175/2008JHM973.1>, 2009.  
573
- 574 Gimeno, L., Vázquez, M., Eiras-Barca, J., Sorí, R., Stojanovic, M., Algarra, I., Nieto, R., Ramos,  
575 A., Durán-Quesada, A.M., & Dominguez, F.: Recent progress on the sources of continental



- 576 precipitation as revealed by moisture transport analysis, *Earth Sci Rev*, 201, 103070,  
577 <http://dx.doi.org/10.1016/j.earscirev.2019.103070>, 2020.
- 578
- 579 González-Carranza, Z., Hooghiemstra, H. and Vélez, M.I. 2012. A 14,000 yr pollen and diatom  
580 based record of environmental and climatic change from South Colombian Andes shows decadal  
581 climate variability. *The Holocene* 22:1227-1241. DOI: 10.1177/0959683612451183, 2012.
- 582
- 583 Haug, G. H., Hughen, K. A., Sigman, D. M., Peterson, L. C., & Röhl, U.: Southward migration  
584 of the intertropical convergence zone through the Holocene, *Science*, 293, 1304-1308,  
585 <http://dx.doi.org/10.1126/science.1059725>, 2001.
- 586
- 587 Hersbach, H., Bell, B., Berrisford, P., Hirahara, S., Horányi, A., Muñoz-Sabater, J., ... &  
588 Thépaut, J. N.: The ERA5 global reanalysis, *Q J Roy Meteor Soc*, 146, 1999-2049,  
589 <http://dx.doi.org/10.1002/qj.3803>, 2020.
- 590
- 591 Hoyos, I., Dominguez F., Cañon-Barriga J., Martínez J. A., Nieto R., Gimeno L., and Dirmeyer  
592 P. A.: Moisture origin and transport processes in Colombia, northern South America, *Clim. Dyn.*,  
593 <http://dx.doi.org/10.1007/s00382-017-3653-6>, 2018.
- 594
- 595 Hooghiemstra, H. & Flantua, S.G.A.: Colombia in the Quaternary: An overview of  
596 environmental and climatic change. In: Gómez, J. & Pinilla-Pachon, A.O. (editors), *The*  
597 *Geology of Colombia, Volume 4 Quaternary*. Servicio Geológico Colombiano, Publicaciones  
598 Geológicas Especiales 38, 52 p. Bogotá. <https://doi.org/10.32685/pub.esp.38.2019.02>, 2019.
- 599
- 600 Hu, S., & Fedorov, A. V.: Cross-equatorial winds control El Niño diversity and change, *Nat*  
601 *Clim Change*, 8, 798-802, <http://dx.doi.org/10.1038/s41558-018-0248-0>, 2018.
- 602
- 603 Jaramillo, D., Velez, M.I., Escobar, J.H., Pardo-Trujillo, A., Vallejo, F., Villegas, J.C., Acevedo,  
604 A.L., Curtis, J., Rincón, H. and Trejos-Tamayo, R.: Mid to late holocene dry events in  
605 Colombia's super humid Western Cordillera reveal changes in regional atmospheric circulation,  
606 *Quaternary Sci Rev*, 261, 106937, <http://dx.doi.org/10.1016/j.quascirev.2021.106937>, 2019.
- 607
- 608 Jiménez-Sánchez, G., Markowski, P. M., Jewtoukoff, V., Young, G. S., & Stensrud, D. J.: The  
609 Orinoco low-level jet: An investigation of its characteristics and evolution using the WRF  
610 model, *J Geophys Res-Atmos*, 124, 10696-10711, <http://dx.doi.org/10.1029/2019JD030934>,  
611 2019.
- 612
- 613 Jones, M., Metcalfe, S., Davies, S., Noren, A.: Late Holocene climate reorganisation and the  
614 North American Monsoon Quaternary, *Sci Rev*, 124, 290-295,  
615 <http://dx.doi.org/10.1016/j.quascirev.2015.07.004>, 2015.



- 616  
617 Karamperidou, C. and DiNezio, P.: Holocene hydroclimatic variability in the  
618 tropical Pacific explained by changing ENSO diversity, *Nat commun*, 13,7244-,  
619 <http://dx.doi.org/10.1038/s41467-022-34880-8>, 2022.  
620  
621 Ledru, M.P., Aquino-Alfonso, O., Finsinger, W., Samaniego, P., and Hidalgo, S.: Changes in the  
622 vegetation and water cycle of the Ecuadorian paramo during the last 5000 years, *The Holocene*,  
623 32, 950-, <http://dx.doi.org/10.1177/09596836221101251>, 2022.  
624  
625 López, M. E., & Howell, W. E.: Katabatic winds in the equatorial Andes, *J Atmos Sci*, 24, 29-35,  
626 [http://dx.doi.org/10.1175/1520-0469\(1967\)024%3C0029:KWITEA%3E2.0.CO;2](http://dx.doi.org/10.1175/1520-0469(1967)024%3C0029:KWITEA%3E2.0.CO;2), 1967.  
  
627 Maraun, D., and Kurths, J.: Cross wavelet analysis: Significance testing and pitfalls, *Nonlinear*  
628 *Process. Geophys.* 11, 505–514, <http://dx.doi.org/10.5194/npg-11-505-2004>, 2004.  
  
629 Marchant, R., Behling, H., Berrio, J.C., Cleef, A., Duivenvoorden, J., Hooghiemstra, H., Kuhry,  
630 P., Melief, B., Van Geel, B., Van der Hammen, T., Van Reenen, G., Wille, M.: Mid to Late-  
631 Holocene pollen-based biome reconstructions for Colombia, *Quaternary Sci Rev* 20, 1289–  
632 1308, [http://dx.doi.org/10.1016/S0277-3791\(00\)00182-7](http://dx.doi.org/10.1016/S0277-3791(00)00182-7), 2001.  
633  
634 Marchant R and Hooghiemstra H.: Rapid environmental change in African and  
635 South American tropics around 4000 years before present: a review. *Earth Sci*  
636 *Rev*, 66, 215-260, <http://dx.doi.org/10.1016/j.earscirev.2004.01.003>, 2004.  
637  
638 Marengo, J. A., and Espinoza, J. C.: Extreme seasonal droughts and floods in Amazonia: causes,  
639 trends and impacts, *Int J Climatol*, 36, 1033-1050, <http://dx.doi.org/10.1002/joc.4420>, 2016.  
640  
641 Martinez, J. A., Arias, P. A., Junquas, C., Espinoza, J. C., Condom, T., Dominguez, F., &  
642 Morales, J. S.: The Orinoco Low-Level Jet and the Cross-Equatorial Moisture Transport Over  
643 Tropical South America: Lessons From Seasonal WRF Simulations, *J Geophys Res-Atmos*, 127,  
644 e2021JD035603, <http://dx.doi.org/10.1029/2021JD035603>, 2022.  
645  
646 Moy, C. M., Seltzer, G. O., Rodbell, D. T., & Anderson, D. M.: Variability of El Niño/Southern  
647 Oscillation activity at millennial timescales during the Holocene epoch, *Nature*, 420, 162-165,  
648 <http://dx.doi.org/10.1038/nature01194>, 2002.  
649  
650 Muñoz, E., Busalacchi, A. J., Nigam, S., & Ruiz-Barradas, A.: Winter and summer structure of  
651 the Caribbean low-level jet, *J Climate*, 21, 1260-1276,  
652 <http://dx.doi.org/10.1175/2007JCLI1855.1>, 2008.  
653



- 654 Noone, D., and I. Simmonds, A three-dimensional spherical trajectory algorithm. Research  
655 Activities in Atmospheric and Oceanic Modelling, Report No. 28, WMO/TD-No. 942. H.  
656 Ritchie, Ed., World Meteorological Organization, 3.26-3.27, 1999.  
657
- 658 Patiño, L.F., Vélez, M.I., Weber, M. Velásquez, C., David, S., Rueda, D., and Castañeda, I.: Late  
659 Pleistocene-Holocene environmental history of a freshwater paramo ecosystem in the Northern  
660 Andes, J Quaternary Sci, 35, 1046–1056, <http://dx.doi.org/10.1002/jqs.3249>, 2020.  
661
- 662 Posada-Marín, J. A., Rendón, A. M., Salazar, J. F., Mejía, J. F., and Villegas, J. C., WRF  
663 downscaling improves ERA-Interim representation of precipitation around a tropical Andean  
664 valley during El Niño: implications for GCM-scale simulation of precipitation over complex  
665 terrain, Clim. Dyn., 1-21, <http://dx.doi.org/10.1007/s00382-018-4403-0>, 2018.  
666
- 667 Poveda, G., and Mesa, O. J.: On the existence of Lloró (the rainiest locality on Earth): Enhanced  
668 ocean-land-atmosphere interaction by a low-level jet, Geophys res lett, 27, 1675-1678,  
669 <http://dx.doi.org/10.1029/1999GL006091>, 2000.  
670
- 671 Poveda, G., Jaramillo, A., Gil, M. M., Quiceno, N., and Mantilla, R. I.: Seasonally in ENSO-  
672 related precipitation, river discharges, soil moisture, and vegetation index in Colombia, Water  
673 Resour Res, 37, 2169-2178, <http://dx.doi.org/10.1029/2000WR900395>, 2001.  
674
- 675 Poveda, G., Mesa, O. J., Salazar, L. F., Arias, P. A., Moreno, H. A., Vieira, S. C., Agudelo P.A,  
676 Toro V.G., and Alvarez, J. F.: The diurnal cycle of precipitation in the tropical Andes of  
677 Colombia, Mon Weather Rev, 133, 228-240, <http://dx.doi.org/10.1175/MWR-2853.1>, 2005.  
678
- 679 Poveda, G., Waylen, P. R., and Pulwarty, R. S.: Annual and inter-annual variability of the  
680 present climate in northern South America and southern Mesoamerica, Palaeogeog, Palaeocli,  
681 234, 3-27, <http://dx.doi.org/10.1016/j.palaeo.2005.10.031>, 2006.  
682
- 683 Poveda, G., Alvarez, D. M., and Rueda, O. A.: Hydro-climatic variability over the Andes of  
684 Colombia associated with ENSO: a review of climatic processes and their impact on one of the  
685 Earth's most important biodiversity hotspots, Clim Dyn, 36, 2233-2249,  
686 <http://dx.doi.org/10.1007/s00382-010-0931-y>, 2011.
- 687 Poveda, G., Jaramillo, L., Vallejo, L.F., 201. Seasonal Precipitation Patterns Along Pathways of  
688 South American Low-Level Jets and Aerial Rivers, Water Resour. Res, 50, 1-21,  
689 <http://dx.doi.org/10.1002/2013WR014087>, 2014.  
690
- 691 Poveda, G., Espinoza, J. C., Zuluaga, M. D., Solman, S. A., Garreaud, R., & van Oevelen, P. J.:  
692 High impact weather events in the Andes, Front Earth Sci, 8, 162-,  
693 <http://dx.doi.org/10.3389/feart.2020.00162>, 2020.





- 694  
695 Poveda, G.: Garantizar la Integridad de los Ecosistemas de Colombia: Condición Básica para  
696 Preservar la Biodiversidad y Desarrollar la Bioeconomía, Departamento Geociencias y Medio  
697 Ambiente. Universidad Nacional de Colombia, Medellín, 2020.  
698  
699 R Core Team. R: A language and environment for statistical computing. R Foundation for  
700 Statistical Computing, Vienna, Austria. URL: <https://www.R-project.org/>, 2021.  
701  
702 Renssen, H.: Climate model experiments on the 4.2 ka event: The impact of tropical sea-surface  
703 temperature anomalies and desertification, *The Holocene*, 32, 378-389,  
704 <http://dx.doi.org/10.1177/09596836221074031>, 2022.  
705  
706 Sachs, J.P., Blois, J.L., McGee1, T., Wolhowe1, M., Haberle, S., Clark, G., and Atahan, P.:  
707 Southward shift of the Pacific ITCZ during the Holocene. *Paleoceanography and*  
708 *Paleoclimatology*, 33, 1383–1395, <http://dx.doi.org/10.1029/2018PA003469>, 2018.  
709  
710 Salas, H. D., Poveda, G., Mesa, Ó. J., & Marwan, N.: Generalized synchronization between  
711 ENSO and hydrological variables in Colombia: A recurrence quantification approach. *Frontiers*  
712 *in Applied Mathematics and Statistics*, 6, 3-, <http://dx.doi.org/10.3389/fams.2020.00003>, 2020.  
713  
714 Schneider, T., Bischoff, T., & Haug, G. H.: Migrations and dynamics of the intertropical  
715 convergence zone. *Nature*, 513, 45-53, <http://dx.doi.org/10.1038/nature13636>, 2014.  
716  
717 Schwalb, A., Dean, W.D., Fritz, S.C., Geiss, C., Kromer, B.: Centennial eolian cyclicity in the  
718 Great Plains, USA: a dominant climate pattern of wind transport over the past 4000 years?  
719 *Quaternary Sci Rev*, 2325-2339, <http://dx.doi.org/10.1016/j.quascirev.2010.06.007>, 2010.  
720  
721 Seillès, B., Sánchez Goñi, M.F., Ledru, M.P., Urrego, D.H., Martinez, P., Hanquiez, V., and  
722 Schneider, R.: Holocene land–sea climatic links on the equatorial Pacific coast (Bay of  
723 Guayaquil, Ecuador), *The Holocene*, 26, 567-577, <http://dx.doi.org/10.1177/0959683615612566>,  
724 2016.  
725  
726 Sierra, J. P., Arias, P. A., Durán-Quesada, A. M., Tapias, K. A., Vieira, S. C., and Martínez, J.  
727 A.: The Chocó low-level jet: past, present and future, *Clim Dynam*, 56, 2667-2692,  
728 <http://dx.doi.org/10.1007/s00382-020-05611-w>, 2021.  
729  
730 Sulca, J., Takahashi, K., Espinoza, J. C., Vuille, M., and Lavado-Casimiro, W.: Impacts of  
731 different ENSO flavors and tropical Pacific convection variability (ITCZ, SPCZ) on austral  
732 summer rainfall in South America, with a focus on Peru, *Int J Climatol*, 38, 420-435,  
733 <http://dx.doi.org/10.1002/joc.5185>, 2018.



- 734  
735 Tedeschi, R. G., Cavalcanti, I. F., and Grimm, A. M.: Influences of two types of ENSO on South  
736 American precipitation, *Int J Climatol*, 33, 1382-1400, <http://dx.doi.org/10.1002/joc.3519>, 2013.
- 737 Torrence, C. and Compo, G.P.: A Practical Guide to Wavelet Analysis, *Bull. Am. Meteorol.*  
738 *Soc.*, 79, 61–78, [http://dx.doi.org/10.1175/1520-](http://dx.doi.org/10.1175/1520-0477(1998)079%3C0061:APGTWA%3E2.0.CO;2)  
739 [0477\(1998\)079%3C0061:APGTWA%3E2.0.CO;2](http://dx.doi.org/10.1175/1520-0477(1998)079%3C0061:APGTWA%3E2.0.CO;2), 1998.
- 740 Toth, L. T. and Aronson, R. B.: The 4.2 ka event, ENSO, and coral reef development, *Clim. Past*,  
741 15, 105–119, <http://dx.doi.org/10.5194/cp-15-105-2019>, 2019.
- 742  
743 Toth, L., Aronson, R., Vollmer, S.V., Hobbs, J.W., Hurrego, D., Cheng, H., Enochs, I.,  
744 Combosch, D.J., van Woesik, R., and Macintyre, I.G.: ENSO Drove 2500-Year Collapse of  
745 Eastern Pacific Coral Reefs, *Science*, 337, 81-84, <http://dx.doi.org/10.1126/science.1221168>,  
746 2012.
- 747  
748 Trenberth, K. E., and Hurrell, J. W.: Decadal atmosphere-ocean variations in the Pacific, *Clim*  
749 *Dynam*, 9, 303-319, <http://dx.doi.org/10.1007/BF00204745>, 1994.
- 750  
751 Trojer, H.: Fundamentos para una zonificación meteorológica y climatológica del trópico y  
752 especialmente de Colombia, *Cenicafé*, 10, 289-373, ISSN: 0120-0275, 1959.
- 753  
754 Urrea, V., Ochoa, A., and Mesa, O.: Seasonality of rainfall in Colombia, *Water Resour Res*, 55,  
755 4149-4162, <http://dx.doi.org/10.1029/2018WR023316>, 2019.
- 756  
757 Wanner, H., Beer, J., Butikofer J., Crowley, T., Cubasch, U., Fluckiger, J., Goosse, H., Grosjean,  
758 M., Joos, F., Kaplan, J., Kuttel, M., Muller, S., Prentice, C.: Solomina, O., Stocker, F., Tarasov,  
759 P., Wagner, M. and Widmann, M.: Mid-to Late Holocene climate change: an overview,  
760 *Quaternary Sci Rev*, 27, 1791-1828, <http://dx.doi.org/10.1016/j.quascirev.2008.06.013>, 2008.
- 761  
762 Whyte, F. S., Taylor, M. A., Stephenson, T. S., & Campbell, J. D. Features of the Caribbean low  
763 level jet. *International Journal of Climatology*, *Q J Roy Meteor Soc*, 28.1, 119-128,  
764 <http://dx.doi.org/10.1002/joc.1510>, 2008.
- 765  
766 Yepes, J., Poveda, G., Mejía, J. F., Moreno, L., & Rueda, C.: CHOCO-JEX: A research  
767 experiment focused on the Chocó low-level jet over the far eastern Pacific and western  
768 Colombia, *B Am Meteorol Soc*, 100, 779-796, <http://dx.doi.org/10.1175/BAMS-D-18-0045.1>,  
769 2019.
- 770



771 Yi, H. and Shu, H.: The improvement of the Morlet wavelet for multi-period analysis of climate  
772 data, *Comptes Rendus Geosci.*, 344, 483–497, <http://dx.doi.org/10.1016/j.crte.2012.09.007>,  
773 2012.  
774  
775 Zemp, D.C., Schleussner, C.F., Barbosa, H.M.J., Van der Ent, R.J., Donges, J.F., Heinke, J.,  
776 Sampaio, G. and Rammig, A.: On the importance of cascading moisture recycling in South  
777 America, *Atmos Chem Phys Discuss*, 14, 17479–17526, [http://dx.doi.org/10.5194/acp-14-13337-](http://dx.doi.org/10.5194/acp-14-13337-2014)  
778 [2014](http://dx.doi.org/10.5194/acp-14-13337-2014), 2014.  
779  
780 Zemp, D.C., Schleussner, C.F., Barbosa, H.M., Hirota, M., Montade, V., Sampaio, G., Staal, A.,  
781 Wang-Erlandsson, L. and Rammig, A.: Self-amplified Amazon Forest loss due to vegetation-  
782 atmosphere feedbacks. *Nature Commun*, 8, 1–10, <http://dx.doi.org/10.1038/ncomms14681>, 2017.  
783  
784  
785  
786  
787  
788  
789  
790  
791  
792  
793  
794  
795  
796  
797  
798  
799  
800  
801  
802  
803  
804  
805  
806  
807  
808  
809  
810